Success and failure of the convection-diffusion model to describe transport in fusion plasmas

D.F. Escande[1,2], F. Sattin[2]

[1] *UMR 7345 CNRS-/Aix-Marseille Université, Marseille, France*

[2] *Consorzio RFX, Associazione EURATOM-ENEA sulla fusione, Padova, Italy*

Understanding the transport of particles, energy, and angular momentum in hot magnetized plasmas is essential to predict and optimize future fusion reactors based on magnetic confinement. The convection-diffusion model (CDM) is the simplest paradigm to describe such a transport. It has been widely used to interpret experiments and has been backed up by a whole series of theoretical approaches [1]. However, the validity of this model to describe perturbative experiments is debated. Some of the results can eventually be reabsorbed within extensions of the CDM, by including suitable pinch terms and/or allowing for sharp differences in transport properties between equilibrium and perturbed plasma states [2,3], whereas some other findings are extraordinarily resilient: the most glaring evidence is provided by heat transport experiments featuring sign inversion of the temperature perturbation during its radial propagation: cold pulses at the edge turn into heating of the core, or *vice versa* [4,5]. Another kind of evidence involves the propagation of heat perturbations produced by two different sources *in the same equilibrium plasma*, featuring mutually incompatible transport modalities [6].

The CDM keeps being widely used, since it is a very flexible model [7]. However, for both the interpretation of experiments and guidance to theoreticians, it is important to know whether this model is not only convenient, but also right in some instances. The issue of the validation of the CDM against experimental data has always been active [3,4,8,9]. However, till now it has been performed in a rather indirect way. Transport codes compute the profile of transport coefficients as follows: the radial profiles of these coefficients are iteratively adjusted until getting the best match between the measured profile of the transported quantity $\xi^{(meas)}$ and its reconstruction by the code through the CDM, $\xi^{(num)}$. The quality of the match is quantified by the functional $F = \sum_{i=1,n} (\xi_i^{(meas)} - \xi_i^{(num)})^2$. The code output is considered as acceptable, and implicitly *a fortiori* the CDM is, if *F* is below the bound provided by the experimental error bars. However, it never happens that *F*=0, and the above algorithm does not provide a way to discern whether $F\neq 0$ is related to the imperfect guess of the transport coefficients, or else to a failure of the CDM. Thus, while experiments provide instances of situations where the CDM fails, the opposite case of a plain success has never been unambiguously shown.

We take here advantage of an alternative way of estimating transport coefficients, the Matricial Approach (MA) [10], that by construction warrants $F=0$. We tackle the analysis of two reference sets of published heat transport experiments. In one case we are able to provide a proof of the non contradiction with experimental data of the CDM by producing independent reconstructions of the heat diffusivity and pinch velocity profiles for different experiments within the same plasma, and showing that they mutually agree within the experimental error bars. Conversely, in another case the same scheme produces an unambiguous instance of a *failure* of the CDM.

The MA assumes that both the driving term (the source S_ω) and the plasma response have a periodic modulation with angular frequency ω; the diffusivity χ and pinch V are solution at each radial point r of the linear system $\mathbf{M}\cdot\mathbf{Y}=\mathbf{\Gamma}$, where

$$\mathbf{Y}=\begin{pmatrix}\chi\\ V\end{pmatrix},\mathbf{M}=\begin{bmatrix}-A'\cos\varphi+A\varphi'\sin\varphi & A\cos\varphi\\ -A'\sin\varphi-A\varphi'\cos\varphi & A\sin\varphi\end{bmatrix},\mathbf{\Gamma}=\begin{pmatrix}W'(r)^{-1}\int_0^r W'(z)\left(\mathrm{Re}\left(S_\omega(z)\right)-\omega A(z)\sin\varphi(z)\right)dz\\ W'(r)^{-1}\int_0^r W'(z)\left(\mathrm{Im}\left(S_\omega(z)\right)+\omega A(z)\cos\varphi(z)\right)dz\end{pmatrix},$$

where $W(r)$ is the volume element, A, φ the measured amplitude and phase of the perturbation. The linear system may be solved where $\det(\mathbf{M})=A^2\,d\varphi/dr$ does not vanish. The error analysis is performed by a Monte Carlo method where the data $\{A_i,\varphi_i\}$ are independently perturbed by random amounts corresponding to the experimental error. For each outcome, smooth approximations $\{A(r),\varphi(r)\}$ are computed and $\chi(r)$ and $V(r)$ are estimated. The corresponding value of F vanishes; therefore, for any given approximation $\{A(r),\varphi(r)\}$, the profiles of $\chi(r)$ and $V(r)$ correspond to an absolute optimum of the reconstruction analysis.

We first consider an experiment carried out at ASDEX-Upgrade [11]. The source was modulated off-axis ECH (placed at $r/a=2/3$) with a square waveform and dominant harmonics at 14.7 Hz. The temperature measurements were performed with a 60-channel ECE heterodyne radiometer. We use the data produced in shot 17175, reported in figures (4,5) of the original paper and reproduced in Fig. (1) here below. Data were fitted using linear combinations of Hermite polynomials. ASDEX geometry is approximated as circular, with minor radius $a=0.65$ m, and electron density was held constant throughout the radius, $n_e = 2{\times}10^{19}$ m^{-3} . The calculation of error bars was done postulating a statistical error of 7% both on the amplitude and the phase; 100 statistical runs were performed.

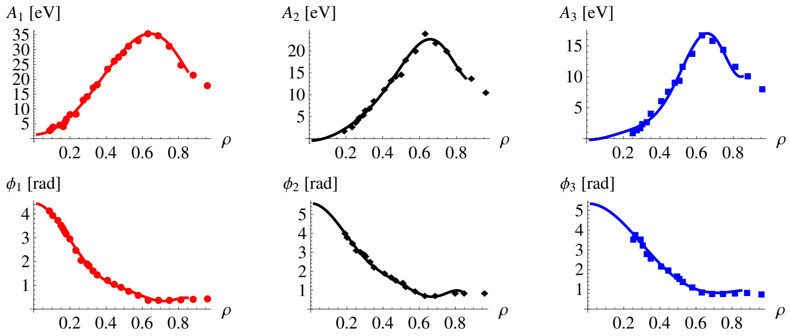

Fig. 1 The symbols stand for raw data, solid curves are examples of fitting functions. From left to right, first, second and third harmonic; upper row, the amplitude, lower row, the phase of the signals.

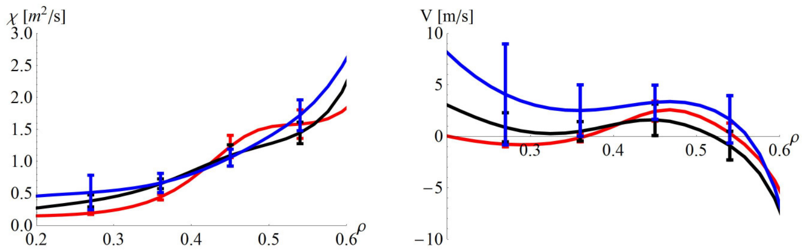

Fig. 2 Left plot, diffusivity; right plot, pinch. The confidence intervals at selected locations are shown, too. Color code is the same of Fig. 1.

The reconstructed profiles are plotted in Fig. (2) They blow off beyond ρ = 0.65, which is the location of the source. In the region 0.3 < ρ < 0.6 the three simulations agree both for the heat pinch and for the diffusivity, which validates the CDM. This validation is especially meaningful thanks to the agreement of three harmonics, and to the high quality of the data which provides small error bars on the profile estimates.

We then consider a perturbative heat transport experiments carried out at JET in discharge 55809: an L-mode plasma with both NBI and off-axis ICR heating (in mode conversion scheme); the latter being located at r/a = 1/3 [6]. A periodic modulation of the ICRH with a square-wave form was applied. Its Fourier analysis shows that just two harmonics are important: ν_1 = 14.5 Hz, and $\nu_3 = 3\ \nu_1$. Temperature fluctuations were measured by a fast ECE radiometer. The measured data are reported in Figs. (1,4) of [6] and here in Fig. (3). We attributed 1 eV normally distributed errors to amplitudes, and 5° uniformly distributed to phases. Figure 4 displays the reconstructed profiles of χ for the two harmonics with the uncertainty band. The two results clearly disagree: the modulation experiment proves the CDM to be irrelevant. The quality of the experimental data provides a strong ground to this statement: an appreciable overlap of the confidence intervals could be achieved only by at least doubling the experimental error. The original paper [6] hinted upon a failure of the Fickian version of the CDM in describing simultaneously the heat modulation and the cold pulse experiment, whereas we show that the former experiment *alone* is sufficient to prove the failure of the CDM, even whenever endowed with the flexibility provided by a pinch velocity independent of the diffusion coefficient. Despite the quantitative disagreement, some qualitative trends are common to both curves. There is a low-transport region below about $\rho = 0.25$, and a large-transport one beyond this radius. This matches the analysis done in [6] where the region above $r/a = 1/3$ was identified as lying on the stability threshold for the onset of stiff transport, with transport enhanced by up a tenfold factor to the equilibrium power-balance value χ_{PB}, while the inner region is stable, with $\chi \approx \chi_{PB}$.

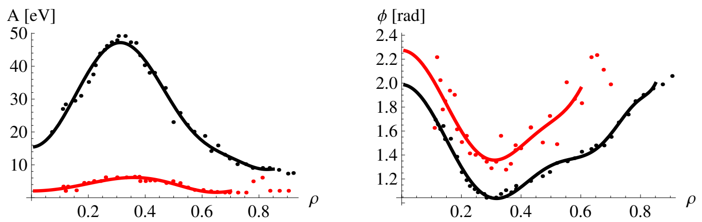

Fig. 3 Data used in the simulation. Black symbols refer to ν_1 harmonic, red ones to ν_3. Left plot, amplitude, right plot, phase. Solid curves are examples of fitting.

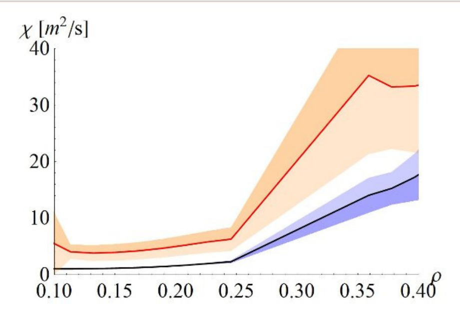

Fig. 4. Diffusivity from the MA from the data in fig. (3), with the same color code. Colored areas stand for the confidence intervals

Acknowledgments.
This work was supported by the European Communities under the Contract of Association between Euratom/ENEA. It benefitted from discussions with P. Mantica

[1] R.J. Goldston, *et al*, in Fusion Physics, Chap. 2 (IAEA 2012); ITER Physics Expert Groups, Nucl. Fusion **39** (1999) 2175
[2] C.M. Bishop and J.W. Connor, Plasma Phys. Control. Fusion **32** (1990) 203
[3] N.J. Lopes Cardozo, Plasma Phys. Control. Fusion **37** (1995) 799
[4] J.D. Callen and M.W. Kissick, Plasma Phys. Control. Fusion **39** (1997) B173
[5] V.D. Pustovitov, Plasma Phys. Control. Fusion **54** (2012) 124036
[6] P. Mantica, *et al*, paper EX/P1-04, 19th IAEA Fusion Energy Conference (Lyon, France, 2002).
[7] D.F. Escande and F. Sattin, Phys. Rev. Lett. **99**, 185005 (2007)
[8] P. Mantica, F. Ryter, C.R. Physique **7** (2006) 634
[9] F. Ryter, R. Dux, P. Mantica and T. Tala, Plasma Phys. Control. Fusion **52** (2010) 124043
[10] K. Krieger *et al*, Nucl. Fusion **30** (1990) 2392; H. Takenaga *et al*, Plasma Phys. Control. Fusion **40** (1998) 183; D.F. Escande and F. Sattin, Phys. Rev. Lett. **108** (2012) 125007; D.F. Escande, *et al*, paper TH/P2-18, 24th IAEA Fusion Energy Conference (San Diego, CA, 2012); F. Sattin, *et al*, Plasma Phys. Control. Fusion **54** (2012) 124025
[11] P. Mantica, *et al*, Plasma Phys. Control. Fusion **48** (2006) 385